

# Progress in the Development of a Detailed Model for Diesel Combustion

R.J.R.Johns

*Ricardo Consulting Engineers Ltd.  
Bridge Works  
Shoreham-by-Sea  
Sussex, BN43 5FG  
England*

## ABSTRACT

The paper describes a detailed model for diesel combustion. The model consists of three main parts, namely: the mean flow and turbulence; the spray dynamics, heat and mass transfer; and the evolution of the composition and temperature fields. For the last of these, a model based on solving equations for the composition joint pdf and associated temperature pdf are presented. This approach has the advantage that it is unnecessary to make a priori assumptions concerning the rate-controlling process as the relative importance of evaporation, turbulent mixing and chemical kinetics is automatically accounted for. To allow a tractable solution of the equations, a simplified representation of the pdf using 7 discrete delta functions for the different fuel, oxidant and products mixed states is proposed.

Initial computations have examined the sensitivity of the computed ignition delay to the diffusivity and compared the delay with experimental data. It is concluded that further theoretical investigations into the effect of physical parameters on the ignition delay are needed to clarify the controlling mechanisms.

## INTRODUCTION

The main events that occur during diesel combustion were identified more than 50 years ago (1). During the intervening years, a number of mathematical models of the combustion process have been proposed and, with varying degrees of success, used to understand the relative importance of the various phenomena involved. However, a generally applicable model does not yet exist and development of a predictive method for diesel combustion remains one of the most difficult tasks facing engine modellers; there are a number of reasons for this. Firstly, many individual processes, including air motion, fuel spray dynamics and evaporation, turbulent mixing, (relatively) low temperature autoignition and high temperature combustion are of importance and none may be ignored if a model is not to be incomplete in one or more respects. Secondly, the mechanisms governing many of these phenomena, such as atomization and detailed chemistry, are either poorly understood or too complicated to be incorporated into a comprehensive model. Finally, it is only in recent years that the computing power required for solving the equation system resulting

from detailed modelling has become generally available.

The combustion model on which the present work is based stems from a series of papers, of which references (2) to (4) are representative, on solving a modelled equation for the evolution of the probability density function (pdf) of reactive scalars. The reader is referred to these works for a detailed description of pdf methods and their application to turbulent, reactive flows. These articles consider the general case of the velocity-composition joint pdf. However, in view of the necessity of retaining reasonably tractable equations for the pdf whilst including models for the spray and chemical kinetics, a simpler variant, namely a composition joint pdf is utilised here.

The purpose of this paper is to describe how a pdf formulation can be applied to diesel combustion and the development and some preliminary results from this model. Although the model cannot yet be regarded as comprehensive, in the respect that some phenomena are not yet represented, for example, no attempt has been made to include either radiative heat transfer or to model any trace emissions, it is sufficiently complete to allow a detailed description and preliminary evaluation.

## CONTENTS OF PAPER

The first section briefly discusses methods for calculating turbulent reactive flows and how a composition joint pdf can be used to describe diesel combustion. Subsequently, the main constituent parts of the model are presented in detail, including: the gas phase mean flow and turbulence fields; the spray dynamics, heat and mass transfer; and the pdf combustion model. These contain a number of important sub-models and the practices adopted for each are discussed. With a model as complicated as this, validation of the individual parts is vital and comparison with experiments and computations of other researchers are described. Finally, a detailed comparison is made with both experimental ignition delay data and other computations using the same autoignition model.

## CALCULATION METHODS FOR TURBULENT REACTIVE FLOWS

### Discussion of Theoretical Methods

The majority of methods for calculating multidimensional, nonpremixed, turbulent reactive flows for engineering purposes have been based on

solving equations for the individual mass fractions. One of the most important terms appearing in these equations is the mean rate of chemical reaction. This has usually been evaluated by assuming that the conversion of reactants into products is determined by the rate of mixing between the various species rather than by chemistry, that is, the fuel, oxidant and products that are in a mixed state are sufficiently hot that chemical kinetics is, by comparison with the rate-of-mixing, "infinitely fast". Fairly simple expressions based on this assumption have been proposed, such as the "eddy break-up" model (5) and its derivatives (6). It is recognised, however, that these expressions are neither generally applicable nor capable of extension, for example, to include chemical kinetics in anything but an approximate fashion.

Other methods have been based on solving equations for the mean and higher order moments of the composition pdf. A minimum of 2 variables are required to describe the composition state for nonpremixed combustion and modelled moment equations are required for the variance of both variables and their co-variance (unless it is assumed that the timescale for chemical reaction is much shorter than that for mixing), in addition to assuming a general form for the pdf - an almost impossible task if all possible cases are to be considered.

By comparison, pdf methods offer a number of potential advantages. Firstly, the term expressing chemical reaction appears in closed form and does not need modelling. Secondly, the relative rates of chemical reaction and turbulent mixing are automatically accounted for and it is therefore unnecessary to assume that one is the rate-controlling process and ignore the other. It is also unnecessary to assume a shape for the pdf or to solve modelled equations for moments, although models for turbulent mixing and transport are required. However, as various processes, in particular, mixing

and chemical reaction, are represented by terms which express transport within composition space, the dimensionality and hence the computational expense of solution increase accordingly.

#### Joint PDF Description of Diesel Combustion.

Figure 1 shows the sequence of the main steps that occur during diesel combustion. Fuel, injected into the combustion chamber, evaporates and mixes with the surrounding hot air. This fuel-air mixture reacts and autoignites to form combustion products. The combustion products subsequently mix with fuel and air and the rate of combustion is then determined mainly by this rate of mixing.

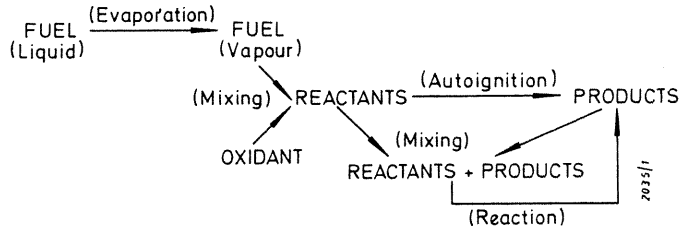


Figure 1. Main steps during diesel combustion.

To illustrate how pdfs can be used to describe diesel combustion, figure 2 shows a sequence of pdfs that might be observed at some position in the cylinder from a time prior to injection to a time when combustion is complete. The symbols "F", "O" and "P" refer to fuel, oxidant and products respectively and these states are located at the vertices of a triangle in composition space. This triangle defines the limits of possible compositions and its sides represent variations in two of the variables in the absence of the third. Compositions within the triangle contain all species. In this simplified

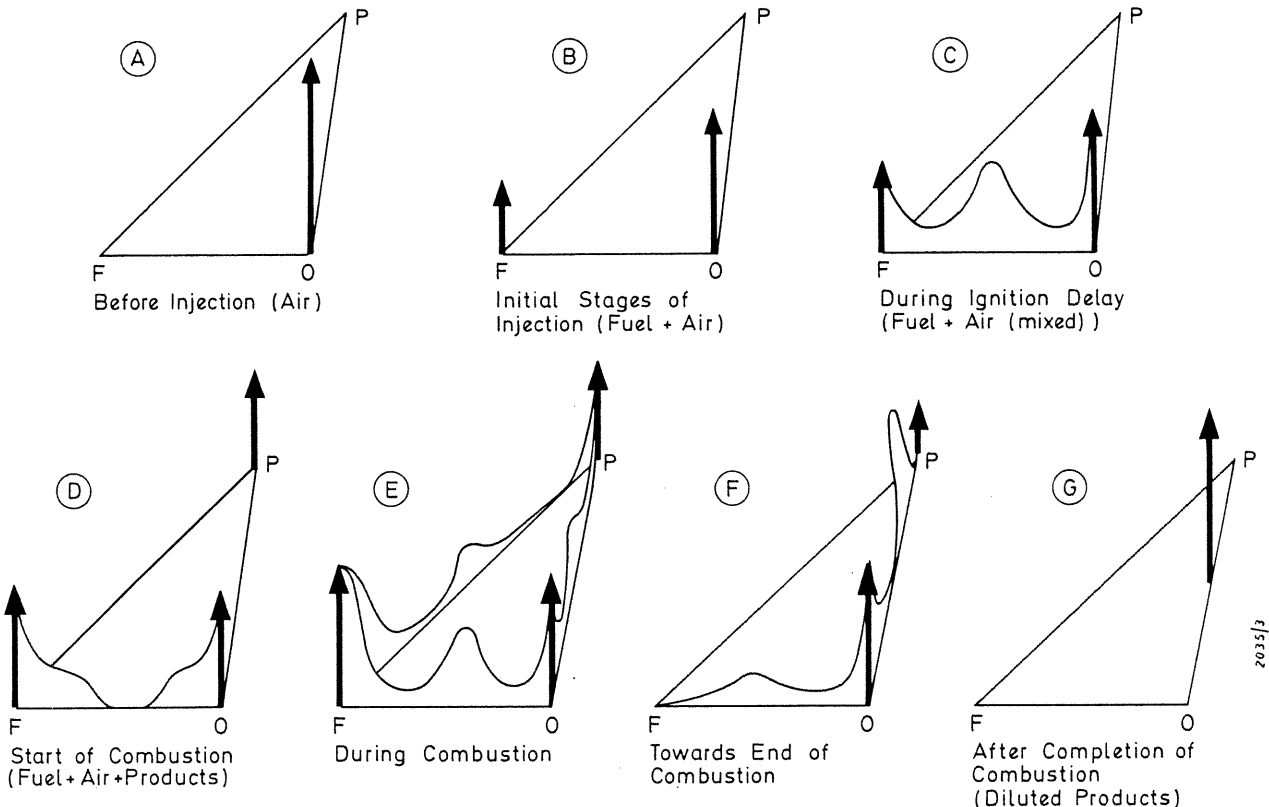


Figure 2. Sequence of typical pdfs during diesel combustion.

fuel-oxidant-products representation, the composition is defined by two independent variables, as discussed later. Experimental determination of such pdfs would be extremely difficult but could, in principle, be achieved by simultaneously measuring fuel concentration and temperature, the latter being highly correlated with products mass fraction. Although such data have been obtained in laboratory flames (7), measurement within an engine cylinder would be considerably more difficult.

The first pdf, depicted in figure 2a, shows a single delta function at the oxidant vertex. This indicates that, before injection (or, at least, before fuel vapour has reached this particular location in the cylinder), the probability of finding oxidant is unity. As the liquid fuel evaporates and is transported by convection and diffusion, a finite probability of fuel and oxidant co-existing is possible, shown in figure 2b. Unless mixing occurs, the fuel and oxidant will remain segregated; the effect of mixing is to produce the pdf shown in figure 2c. While evaporation and mixing continue, the fuel-air mixture that has already formed undergoes chemical reactions leading to autoignition. When this occurs, the effect is to convert the fuel-air mixture into products, shown in the pdf of figure 2d.

After ignition, combustion products are available for mixing with the other states and combustion continues, controlled primarily by the rate of mixing, which determines the rate at which a hot, reactive fuel-air-products mixture can be formed. Figures 2e and 2f show pdfs that would be expected during this period. After combustion and mixing of the combustion products with any residual air is complete, the composition can be represented by the products-oxidant composition shown in figure 2g.

It should be noted that temperature would be strongly correlated with the different states, thus, the initial oxidant temperature would be, typically, 800 K, the fuel temperature 500 - 600 K, and the products, 2500 K, with the various mixed composition states at intermediate values.

The above sequence of events describes "normal" combustion and, whilst this is of interest, there are a number of limiting cases which are probably of even greater interest because of their importance for abnormal combustion. The first of these, shown in figure 3a, is for a low cetane number fuel. Here, an adequate quantity of fuel has

evaporated and mixed with the surrounding air but has failed to ignite. The amount of energy released when ignition does finally occur is proportional to the amount of fuel-air mixture, hence the high "premixed" peak in the heat release rate diagram associated with these conditions.

Figure 3b shows the form of the pdf expected under conditions when the combustion is limited by mixing. There is sufficient fuel, oxidant and products and any fuel-oxidant-products mixture that is formed reacts to form more products on a time scale that is much shorter than that of the mixing. In contrast, if the temperature falls or intense mixing occurs such that chemical kinetics becomes the rate-controlling process, the pdf depicted in figure 3c would be expected. In this situation, mixing continues to form a fuel-oxidant-products mixture but its temperature is too low for rapid chemical reaction to convert the fuel-oxidant into further products. Under these conditions there is a possibility of quenching.

#### MATHEMATICAL DESCRIPTION OF THE MODEL

##### Main Sub-Models

The number and complexity of the different processes involved in modelling diesel combustion requires a certain discipline in the development and subsequent assembly of the various constituent parts. The approach adopted here has been to develop and validate each sub-model separately wherever possible. This has a number of advantages, including: confidence that each sub-model is behaving as expected (at least in isolation); a modular program structure, allowing clear interfaces between the various sub-models; and the ability to activate, suppress or run alternative sub-models without making program changes.

The complete model consists of a number of distinct but communicating major sub-models, these being:

- 1) The dynamics of the gas-phase: determination of the mean flow and turbulence fields.
- 2) The dynamics, heat and mass transfer of the fuel spray.
- 3) The transport, mixing and chemical reaction, which determines the composition and temperature fields.

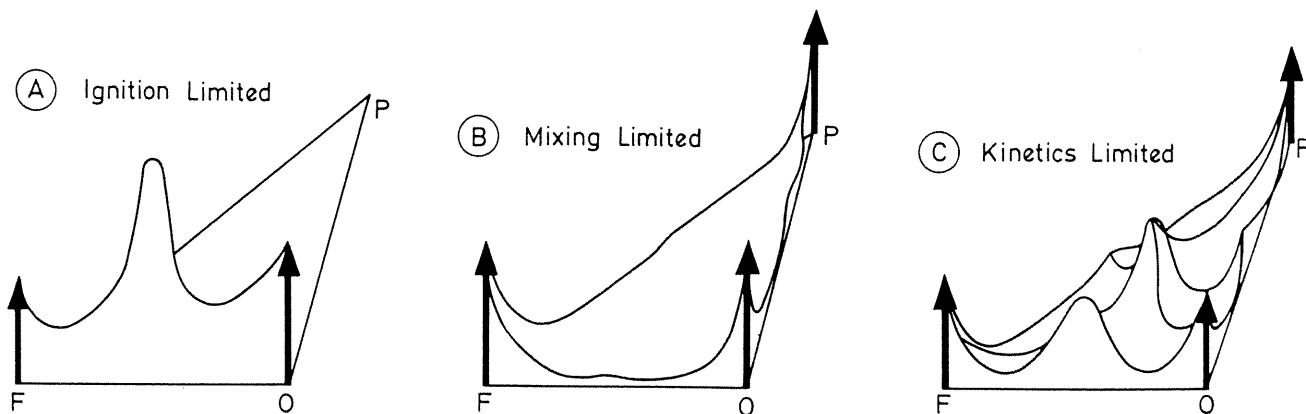


Figure 3. PDFs illustrating different rate-limiting processes.

The sub-models associated with each are discussed in more detail below.

#### Gas Phase Dynamics.

The gas phase mass, momentum and energy conservation equations may be expressed as:

$$\frac{\partial \bar{\rho}}{\partial t} + \frac{\partial}{\partial x_i} (\bar{\rho} U_i) = S_m \quad (1)$$

$$\frac{\partial \bar{\rho} U_j}{\partial t} + \frac{\partial}{\partial x_i} (\bar{\rho} U_i U_j) = - \frac{\partial \tau_{ij}}{\partial x_i} - \frac{\partial \bar{p}}{\partial x_j} + S_u \quad (2)$$

$$\frac{\partial \bar{\rho} \tilde{h}}{\partial t} + \frac{\partial}{\partial x_i} (\bar{\rho} U_i \tilde{h}) = - \frac{\partial J_i^h}{\partial x_i} + \frac{\partial \bar{p}}{\partial t} + S'_h + S''_h \quad (3)$$

where a tilde denotes a density-weighted, ensemble-averaged value;  $\bar{\rho}$  is the product of the mean gas density and the void fraction;  $\tilde{U}_i$  is the velocity in direction  $x_i$ ;  $\tau_{ij}$  is the stress tensor and includes both the turbulent and viscous contributions;  $\bar{p}$  is the pressure;  $\tilde{h}$  is the stagnation enthalpy;  $J^h$  is the turbulent and viscous diffusive energy flux;  $S_m$  is a mass source arising through fuel evaporation;  $S_u$  is the momentum exchange between the spray and the gas phase;  $S'_h$  and  $S''_h$  are energy sources or sinks and are the contributions from chemical heat release and fuel evaporation respectively.

The turbulent fluxes of momentum and heat are modelled with a gradient diffusion approximation where the turbulent exchange coefficient is determined from the  $k - \epsilon$  model, the equations of the latter being:

$$\begin{aligned} \frac{\partial \bar{\rho} k}{\partial t} + \frac{\partial}{\partial x_i} (\bar{\rho} U_i k) = - \frac{\partial J_i^k}{\partial x_i} \\ + \mu_i G_{ij} - \frac{2}{3} \frac{\partial \sigma_m}{\partial x_m} \left[ \mu_i \frac{\partial \sigma_m}{\partial x_m} + \bar{\rho} k \right] - \bar{\rho} \epsilon \end{aligned} \quad (4)$$

$$\begin{aligned} \frac{\partial \bar{\rho} \epsilon}{\partial t} + \frac{\partial}{\partial x_i} (\bar{\rho} U_i \epsilon) = - \frac{\partial J_i^\epsilon}{\partial x_i} \\ + C_1 \frac{\bar{\rho} \epsilon}{k} \left\{ \mu_i G_{ij} - \frac{2}{3} \frac{\partial \sigma_m}{\partial x_m} \left[ \mu_i \frac{\partial \sigma_m}{\partial x_m} + \bar{\rho} k \right] \right\} \\ - C_2 \frac{\bar{\rho} \epsilon^2}{k} + C_3 \bar{\rho} \epsilon \frac{\partial \sigma_m}{\partial x_m} \end{aligned} \quad (5)$$

where  $k$  and  $\epsilon$  are the turbulent kinetic energy (tke) and its dissipation rate respectively;  $G_{ij}$  is the generation rate of tke. Constants appearing in these equations are assigned values in accordance with the recommendations of (8).

#### Fuel Spray Dynamics, Heat and Mass Transfer

During the past decade, the Discrete Droplet Model (DDM) has become firmly established for modelling spray dynamics in engines. Since the early work described in (9,10) a considerable amount of refinement and validation has taken place. No attempt will be made to review the accomplishments of the various researchers, however, the practices adopted here and the reasons for their choice are discussed.

The DDM is based upon a Monte Carlo solution of the spray equation. This, in its most general form, has 8 dimensions (3 space, 3 droplet velocity, size and temperature) and solution by conventional discretisation of the 8-dimensional space is therefore impractical. In the DDM the spray is represented by an ensemble of droplet parcels. These

are introduced at the injector (in practice, slightly downstream of the nozzle hole) throughout the injection period with initial conditions determined from a specified injection rate, spray angle and droplet size distribution, although these last two quantities may be correlated with injector geometry and operating conditions. Each droplet parcel contains a number of identical, non-interacting droplets such that the characteristics of a single member define the characteristics of the parcel. Providing the number of droplet parcels is statistically representative, the characteristics of the ensemble of parcels represent the characteristics of the spray.

The behaviour of a single droplet parcel is determined from solution of a system of ordinary differential equations (see, for example, (11)) for the parcel's position ( $y_i$ ), velocity ( $u_i$ ) diameter ( $d$ ) and temperature ( $T_1$ ), as follows:

$$\frac{dy_i}{dt} = u_i \quad (6)$$

$$\frac{du_i}{dt} = \frac{3}{4} C_D \frac{\rho_g}{\rho_l} \frac{1}{d} U_R (U_i - u_i) \quad (7)$$

$$\frac{d(\rho \pi d^3 / 6)}{dt} = \dot{m} - \pi d D_{12} \rho \ln \left\{ \frac{P - P_{v,\infty}}{P - P_{v,s}} \right\} Sh \quad (8)$$

$$\frac{d(C_p T \rho \pi d^3 / 6)}{dt} = \pi d K (T_g - T_1) f(z) Nu + \dot{m} H_{fg} \quad (9)$$

where  $f(z) = z/(e^z - 1)$ ;  $z = C_p \dot{m} / (\pi d K Nu)$ ;  $C_D$  is the drag coefficient;  $U_R$  the relative velocity between gas and droplet;  $D_{12}$  the diffusion coefficient;  $K$  the thermal conductivity;  $Sh$  and  $Nu$  the Sherwood and Nusselt Numbers respectively;  $H_{fg}$  the latent heat of vapourisation; and subscripts  $v$  and  $l$  refer to the vapour and liquid phases respectively whilst  $\infty$  and  $s$  refer to the values evaluated in the surroundings and at the droplet surface.

As a droplet parcel traverses a mesh cell, it exchanges mass, momentum and energy with the gas phase. Thus, at the same time that equations (6) to (9) are solved, the terms  $S_m$ ,  $S_u$  and  $S'_h$  in equations (1) to (3) are assembled. In addition to the interactions of the droplet parcels with the mean flow, they are also affected by other phenomena, as discussed below.

Droplet-Turbulence Interactions. Equations (6) and (7) describe the behaviour of a droplet in a field of gas velocity  $\underline{U}$ , however, the turbulence modulates the droplet's trajectory according to the level of turbulent fluctuations. Various models have been proposed to account for this based on the interaction of a droplet with a turbulent eddy. The variant used here is that described in (12), where further details can be found. In general, the effect of droplet-turbulence interactions is to increase the lateral spreading rate of the jet, as the droplets migrate from a region of high turbulence, near the jet centreline, to lower turbulence near the periphery.

Droplet-Droplet Interactions. Interaction between droplets are of most importance where they are most densely packed, that is, close to the nozzle. The most comprehensive work on droplet-droplet interactions in diesel sprays is that described in (13); this model is used, without change, in the present calculations.

Secondary Droplet Breakup. Models for secondary droplet breakup have been proposed (14,15) based on the oscillation modes of unstable droplets. The model in reference (15) has been implemented but has not been used in the calculations presented here to allow comparison with previous computations (22) of ignition delay.

Droplet Parcel Introduction. It has been found that the droplet parcel introduction procedure, that is, specification of the initial conditions, plays a crucial role in determining the subsequent spray behaviour. It is important that droplet parcels are introduced some distance downstream of the nozzle exit plane to avoid unrealistic behaviour of the collision model. As indicated in (13), the equations are invalid for the flow regime close to the nozzle and the practice adopted here is similar to that of (13) whereby it is assumed that the spray spreads at the initial spray angle to a distance downstream where the void fraction is 0.1, and that the gas and liquid are in equilibrium there. Source terms,  $S_{\alpha}$ , are determined to ensure that overall momentum is conserved. The initial mean droplet size is determined according to the recommendations of (16) whilst the distribution is assumed to be the same as that found downstream in the experiments of (17).

PDF COMBUSTION MODEL

General Description

A transport equation for the composition joint pdf has been derived in (4). If there is also a source or sink of one of the scalars resulting from phase change, this equation is:

$$\begin{aligned} & \frac{\partial}{\partial t} [\bar{\rho} \mathcal{P}(\Psi)] + \frac{\partial}{\partial x_i} [\bar{\rho} U_i \mathcal{P}(\Psi)] - \frac{\partial}{\partial x_i} \left[ \Gamma_i \frac{\partial \mathcal{P}(\Psi)}{\partial x_i} \right] \\ & + \frac{\partial}{\partial \Psi_{\alpha}} \left[ \frac{1}{\rho} \frac{\partial J_{\alpha}^{\prime}}{\partial x_i} \bar{\rho} \mathcal{P}(\Psi) \right] - \frac{\partial}{\partial \Psi_{\alpha}} [\bar{\rho} \mathcal{P}(\Psi) S_{\alpha}^{\prime}(\Psi)] \\ & \qquad \qquad \qquad \text{I} \qquad \qquad \qquad \text{II} \\ & + \frac{\partial}{\partial \Psi_{\alpha}} [S_m \Psi \mathcal{P}(\Psi) - \bar{\rho} \mathcal{P}(\Psi) S_{\alpha}^{\prime\prime}(\Psi)] \qquad \qquad \qquad \text{III} \end{aligned} \quad (10)$$

where  $\bar{\mathcal{P}}(\Psi)$  is the density-weighted joint pdf of species  $\Psi$ ;  $S_{\alpha}^{\prime}(\Psi)$  is a source or sink of  $\Psi$  from chemical reaction;  $S_{\alpha}^{\prime\prime}(\Psi)$  is a source of  $\Psi$  resulting from evolution of fuel vapour from the spray. This is similar to equations (1) to (5) in the respect that it contains time and spatial derivatives and turbulent transport has been modelled by assuming gradient diffusion. However, terms I to III do not have analogous counterparts and these express the effects resulting from transport of  $\bar{\mathcal{P}}(\Psi)$  in  $\Psi$  space. The effect of terms I to III is to increase the dimensionality of the equation by the number of variables used to represent composition space. The minimum number of composition variables required to represent non-premixed combustion is two, as discussed earlier.

Although Monte-Carlo methods, such as that described in (3), are the only feasible approach to solving pdf equations of high dimensionality (> 2 variables), they suffer from the disadvantage that the statistical error decreases slowly with

increasing number of pdf elements ( $1/\sqrt{N}$ ). As a few hundred elements per spatial mesh cell are required to achieve tolerable statistical convergence of even the low order moments, the computing resources can still be considerable for problems in 3 space dimensions.

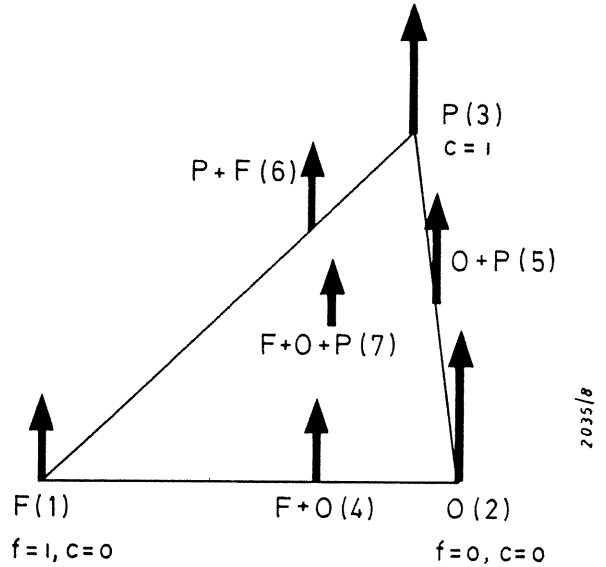
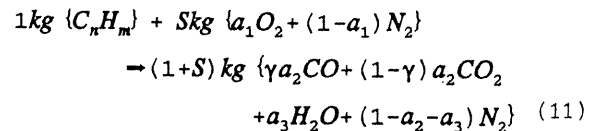


Figure 4. Simplified representation of the pdf.

A conventional grid-based discretisation of composition space is feasible for two composition variables, but in the present stage of development of the method, a simplified representation of the pdf has been used, shown in figure 4. Here, discrete delta functions, referred to as elements and numbered from 1 to 7, are located at the fuel, oxidant and products vertices (1 to 3), along the fuel-oxidant, fuel-products and oxidant-products boundaries (4 to 6) and in the region where fuel-oxidant-products co-exist (7). The elements can be thought of as representing the mass fractions of the various mixed states of fuel, oxidant and products. Also indicated in figure 4 are the independent variables (f) and (c), used to define the 2-dimensional composition space. These quantities are the mass fractions of burned and unburned fuel (f) and the mass fraction of products (c). If reaction proceeds according to the equation:



where

$$\left. \begin{aligned} & a_1 = \text{mass fraction of oxygen in air} \\ & S = \{48n(14-3\gamma) / (21+12\gamma) + 8m\} / \{a_1(12n+m)\} \\ & a_2 = n / \{(12n+m)(1+S)(\gamma/28 + (1-\gamma)/44)\} \\ & a_3 = 9m / \{(12n+m)(1+S)\} \end{aligned} \right\} \quad (12)$$

and  $\gamma/(1-\gamma)$  is the ratio of CO to CO<sub>2</sub>, then the two scalars f and c are related to the mass fractions

of the various species by the following expressions:

$$\left. \begin{aligned} m_{FU} &= f - c/(1+S) \\ m_{O_2} &= a_1(1-f) - cS/(1+S) \\ m_{N_2} &= (1-a_1)(1-f) \\ m_{H_2O} &= a_3c \\ m_{CO} &= \gamma a_2c \\ m_{CO_2} &= (1-\gamma)a_2c \end{aligned} \right\} \quad (13)$$

In general, all of the elements (with the sole exception of element 1) may contain all species. Thus, the designation "fuel + oxidant", for example, is used to identify the particular element whose main constituent species are fuel and oxidant, although the element may also contain small amounts of species found in combustion products (i.e. H<sub>2</sub>O, CO and CO<sub>2</sub>), in this case arising from the autoignition model. The "products" element, 3, is defined as containing only products + fuel or products + oxidant as the case of pure products only exists for stoichiometric combustion. The terms I to III in equation (10) represent the processes of mixing, chemical reaction and generation of  $\Psi$  and are discussed in more detail below.

#### Mixing

Term I represents the effects of molecular mixing and has been discussed at length in (18). The binary mixing model of (19) is used here.

The 7 elements of the pdf contain all possible combinations of mixed fuel, oxidant and products. The general rules governing the outcome of two elements involved in a mixing process are that species are conserved and the mean composition remains unchanged. Thus, for example, fuel (element 1) and oxidant (element 2) mix to form fuel + oxidant (element 4). Similarly, fuel (element 1) and fuel + oxidant (element 4) mix to form more fuel + oxidant, although the resulting contribution to element 4 would be fuel-rich. There are three types of pdf element, namely: elements 1 to 3, located at vertices and containing primarily fuel, oxidant or products; elements 4 to 6, located along boundaries and containing any two of these quantities; and element 7 containing all quantities. This leads to a system of ordinary differential equations governing the mixing of any species,  $s$ , contained within the different element types. For example, for element 1:

$$\frac{dP_{1,\beta}}{dt} = -RP_{1,\beta}(1-P_1) \quad (14)$$

and similarly for elements 2 and 3. Here,  $P_{1,\beta}$  is the probability of species  $s$  in element 1 and  $P_1$  is the probability of element 1. The tilde has been dropped to simplify the notation. Here,  $R$  is a rate of mixing and has dimensions of (1/t). For element 4, the equivalent equation is:

$$\begin{aligned} \frac{dP_{4,\beta}}{dt} &= R(-P_{4,\beta}(1-P_4) \\ &+ P_1 P_{2,\beta} + P_{1,\beta} P_2 + P_4 P_{1,\beta} \\ &+ P_{4,\beta} P_1 + P_2 P_{4,\beta} + P_{2,\beta} P_4) \end{aligned} \quad (15)$$

and similarly for elements 5 and 6. Finally, for

element 7, the equation reads:

$$\begin{aligned} \frac{dP_{7,\beta}}{dt} &= R \left( P_7 \sum_{m=1}^{m-6} P_{m,\beta} \right. \\ &+ P_1 P_{5,\beta} + P_{1,\beta} P_5 + P_2 P_{6,\beta} + P_{2,\beta} P_6 \\ &+ P_4 P_{3,\beta} + P_{4,\beta} P_3 + P_5 P_{4,\beta} + P_{5,\beta} P_4 \\ &\left. + P_6 P_{5,\beta} + P_{6,\beta} P_5 + P_4 P_{6,\beta} + P_{6,\beta} P_4 \right) \end{aligned} \quad (16)$$

Equations for the total element probabilities are obtained by summing over all species within the element, for example, for element 1:

$$\frac{dP_1}{dt} = \sum_{n=1}^{n-6} \frac{dP_{1,n}}{dt} = -RP_1(1-P_1) \quad (17)$$

#### Chemical Reaction.

The effect of chemical reaction on the pdf, represented by term II in equation (10), is to transport probability through  $\Psi$  space towards the products vertex. There are two main aspects of chemical reaction which need to be considered here, namely the (relatively) low temperature autoignition and the high temperature main combustion. A similar delineation has been made in (20) in the context of knock in gasoline engines and is necessary in both the absence and feasibility of using a single kinetics scheme capable of representing the entire process.

**Autoignition.** Reactions leading to autoignition are considered to occur in only the fuel + oxidant element, 4, of the pdf. Clearly, reaction cannot occur in any elements which are deficient in either fuel or oxidant and element 3 is sufficiently hot that autoignition reactions become irrelevant. Element 7 could provide conditions which allow autoignition, however, its composition is assumed to be governed by a high temperature reaction scheme, described later.

The Shell Knock model (21), which has been previously incorporated in multidimensional models for both gasoline engine knock (20) and diesel autoignition (22) is used here to model the autoignition kinetics. This model is based on a degenerate branched chain mechanism using generic intermediate species of  $R$  (radicals),  $B$  (branching agent) and  $Q$  (an intermediate). The kinetics scheme contains initiation, propagation, branching and termination steps and these result in a system of ordinary differential equations for the concentrations of the aforementioned variables, the fuel and for heat release. The oxidant and products concentrations are related algebraically to the other concentrations with an assumed CO/CO<sub>2</sub> ratio in the products.

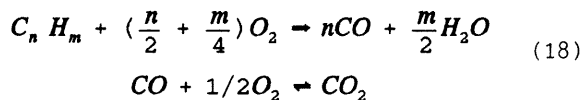
The adaptation of this scheme for incorporation into a multidimensional model is similar to that of (20) and (22) in the following respects: the generic species are assigned molecular weights in accordance with an assumed real composition; they are the dependent variables of transport equations (although as they constitute part of element 4, they also undergo a mixing process and actually obey equation (10)); and they appear in the mass balance for element 4 and hence overall mass conservation.

Autoignition is assumed to have occurred if either the rate of temperature rise exceeds 10<sup>7</sup> K/s or the temperature of element 4 rises above 1200 K.

On detection of autoignition, all fuel or oxidant in the element is burned to form products and the probability associated with element 4 is transported to element 3.

**Main Reaction Kinetics.** Combustion can occur in any of the elements which contain fuel, oxidant and products, namely elements 3, 5, 6 and 7. Whilst it might not be immediately obvious why elements 3, 5 and 6 should burn, as they would appear to be deficient in either one or both of fuel and oxidant, consider the following example: combustion of a fuel-rich mixture has already occurred, resulting in element 3 (products) containing fuel in addition to the usual products of combustion. Element 3 now mixes with element 2 (oxidant), so producing an element 5 contain fuel, oxidant and products. Thus, element 5 may react to form more products.

One of the advantages of the pdf formulation is that realistic reaction rates may be used, in contrast to calculations, albeit for gasoline engines, which have attempted to use artificially reduced reaction rates to try and match experimental burn rates. Although a kinetics scheme of arbitrary complexity may be used, there seems little point in introducing complex kinetics at the present time. Thus, a two step mechanism of the form:



is used in conjunction with the reaction rate data of (23). These data have been used because of their ability to reproduce laminar flame speeds for a range of equivalence ratios and for providing a reasonable estimate of  $[CO]/[CO_2]$  and adiabatic flame temperature. Heat release is associated with the CO oxidation step.

**Evaporation.** Fuel evaporation affects the pdf via term III of equation (10). The two parts of this term account for the increase in probability of element 1 and the corresponding reduction in the probability of the other elements. In practice, this is achieved by addition of the source into element 1 followed by renormalisation of the pdf to unity.

**Thermal Energy Equation.** An equation similar to (10) can be derived expressing energy conservation for the pdf. In addition to the spatial transport, mixing, reaction, and spray source terms, the pressure-work term  $(\partial p/\partial t)$  also appears, as in the global energy equation, (3). Strictly speaking, the latter is not required as energy conservation is expressed by the energy equation for the individual pdf elements (summation over all pdf elements yields equation (3)). However, it is retained for the numerical solution. In this equation, the spray interaction terms need careful treatment to ensure the correct energy exchange between the droplets and the different elements of the gas phase.

#### Method of Solution.

Lack of space precludes a detailed description of the solution method of the equations presented above, however a few general comments will be made. The equations pertaining to each major sub-model are solved sequentially with variables of the other sub-models held constant. Thus, for example, the ordinary differential equations (6) to (9) for the spray are solved with fixed gas velocity,

turbulence, temperature and composition fields. Spatial derivatives appearing in equations (1) to (5) and (10) are approximated with a combination of upwind and central differencing for the convective and diffusive terms respectively. These equations are solved with an implicit numerical scheme.

The equations of the various sub-models of the pdf combustion model are solved sequentially in a similar fashion to that used in the Monte-Carlo method described in (3). Various equation solving methods are employed as appropriate for the different ordinary differential equation systems, including: a Runge-Kutta Merson for the equations of the spray (6) to (9) and the mixing model (14) to (17); and backward differentiation formulae (see, for example, (24)) for the equations of the autoignition and main reaction chemistry, both of which exhibit stiffness. All equation solvers maintain the solution within prescribed error levels.

#### ASSESSMENT OF THE MODEL

##### Validation

As previously mentioned, the software associated with each sub-model has been developed to allow a modular structure for the program. One of the advantages accruing from this approach is the ability to test many of the individual parts in isolation of the others; this must be regarded as a necessary, but not sufficient, condition that the whole is performing correctly. Many of these tests are degenerate cases of the various sub-models and are not reported here. However, comparison with various experimental data has also allowed an evaluation of different aspects of the model and those of relevance are mentioned briefly below.

**Air Motion.** Comparison has been made with unreported LDA data taken at Ricardo in an optically-accessed Hydra research DI diesel engine operating at 2400 rev/min. Figure 5 shows a comparison of the measured and calculated radial and swirl components

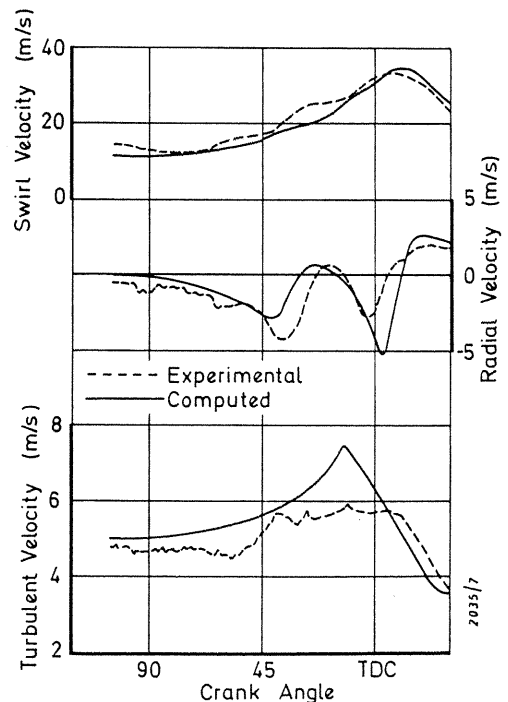


Figure 5. Comparison between measured and computed mean and rms turbulent velocities in a motored engine.

of the mean velocity and the rms turbulent velocity through the compression stroke at an approximately mid-radius, mid-depth location within a re-entrant bowl. These results are representative of the overall level of agreement.

**Spray Model.** Spray penetration is a relatively insensitive parameter to many aspects of the spray model, thus, failure to procure good agreement with experiment would signal a serious deficiency of the model. Three sets of experimental data (25,26,27) for non-evaporating sprays have been used for comparison and the results of these are shown in figures 6 to 8. The behaviour of the droplet interaction model has also been examined for the last set of data, for which similar results to those reported in (13) were obtained. Comparison with both experiments and calculations of the evaporation rate of a single diesel droplet produced results in agreement with those in (28).

**Combustion.** Operation of the autoignition model has been checked by reference to the results reported by its originators (21), where good agreement for the ignition delays of RON 90, 100 and 70 fuels was obtained. The two-step scheme used for

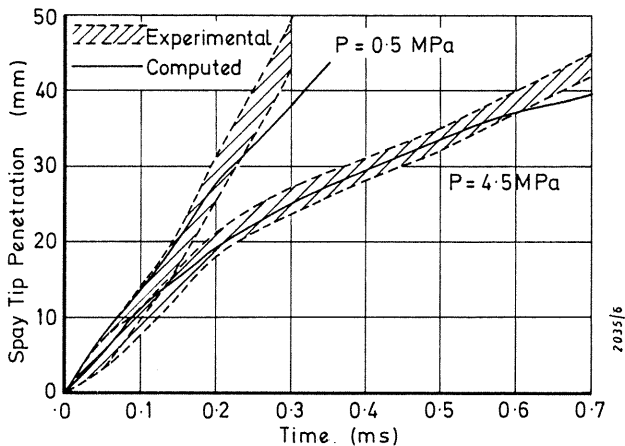


Figure 6. Comparison of computed spray tip penetration with the measurements of ref. (25).

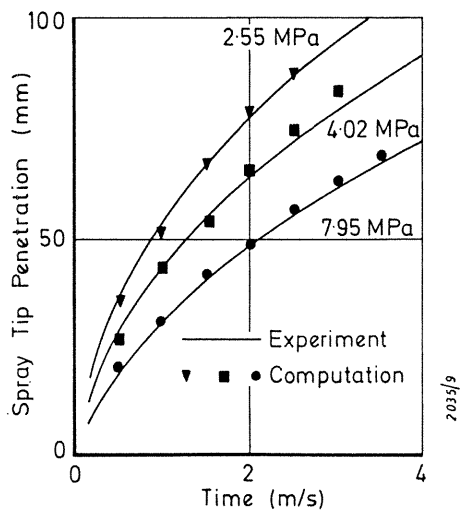


Figure 7. Comparison of computed spray tip penetration with the measurements of ref. (26).

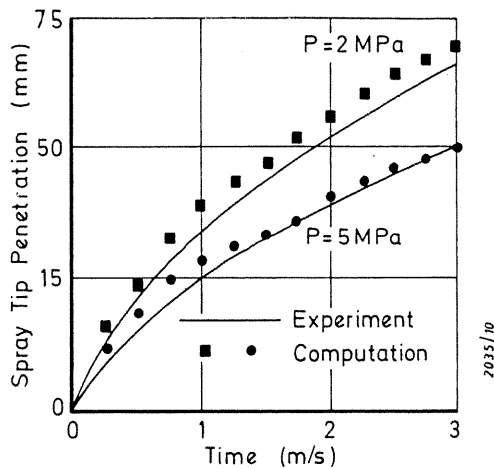


Figure 8. Comparison of computed spray tip penetration with the measurements of ref. (27).

the main combustion kinetics has been tested with rate parameters for methane to ensure agreement with the adiabatic flame temperature and  $[CO]/[CO_2]$  ratio calculations of (23).

**Comparison with Experimental and Calculated Ignition Delay**

The main purpose of this initial evaluation of the model has been to examine the ability to match ignition delay data from both measurements (29) and previous calculations (22). The experimental data were obtained with a heated bomb and with a range of fuels and operating conditions. The data of interest here are for dodecane and with bomb pressures of 10, 20 and 30 bar and temperatures of 670, 750 and 880 K.

The work reported in (22) described how the Shell knock model (21) has been adapted and incorporated into the KIVA program to allow computation of autoignition for diesel and diesel-like sprays. Comparison between the computations of (22) and the measurements of (29) is shown in figure 9. Of particular interest in this study, the

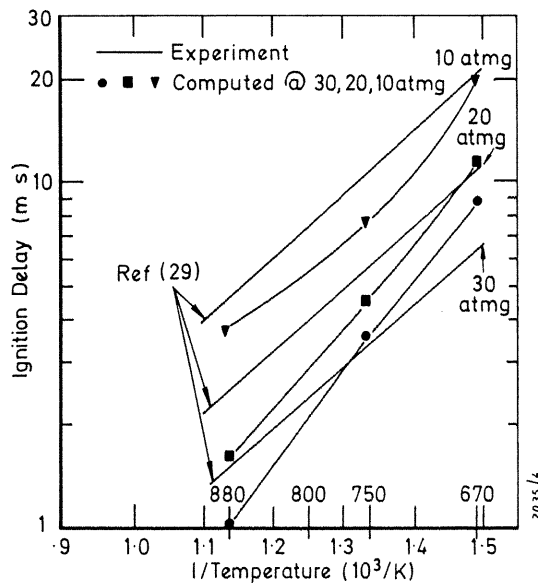


Figure 9. Comparison between computed ignition delay of ref. (22) with the measurements of ref. (29).



sensitivity of the ignition delay to various physical parameters was examined, including the droplet size, fuel vapour pressure and diffusivity. It was found that halving of the droplet size reduced the ignition delay by 30% whereas the delay was insensitive to an artificial reduction in fuel vapour pressure. The computations showed that a factor of 2 change in fuel vapour pressure resulted in only a 20% change in evaporation rate, indicating the evaporation process is mixing limited. It was argued that the higher momentum exchange rate associated with the smaller droplet size produced faster mixing and that the ignition delay was controlled by the rate of mixing. Changes in diffusivity of 20% around the prescribed baseline value of  $0.001 \text{ m}^2/\text{s}$ , however, produced little change in the computed delay. If mixing were the rate-controlling process then it would be expected that the delay would be sensitive to the diffusivity. It was suggested in (22) that this apparent insensitivity was caused by the numerical diffusivity being approximately an order of magnitude greater than the prescribed physical diffusivity.

The results presented here support the proposal in (22) that, for the conditions of these experiments, turbulent transport is important; however it is unlikely to be the only physical process affecting the delay. Initial computations of these sprays with the  $k - \epsilon$  model revealed that the computed diffusivity was typically a factor of 6 greater near the jet centreline than the fixed value of  $0.001 \text{ m}^2/\text{s}$  specified in (22) and double this value near the jet periphery. To try and clarify the effect of diffusivity on the ignition delay, a series of calculations was performed with a fixed diffusivity. To eliminate any effects due to mixing between the fuel and oxidant and allow comparison with the results of (22), the initial composition (air) and temperature were associated with element 4 (fuel + oxidant) rather than element 1 and a large value of the mixing rate ( $R$  in equations (14) to (17)) was specified to ensure rapid mixing. The computational mesh and the droplet parcel introduction rate (800 parcels/ms) are the same as in (22).

Figure 10 shows the variation of ignition delay with diffusivity in the range  $0.001 \text{ m}^2/\text{s}$  to  $0.1 \text{ m}^2/\text{s}$  for two different cases, namely 30 bar/880 K and 20 bar/750 K. The Monte-Carlo solution for the spray introduces some variability into the results, thus, each condition has been repeated 3 times with a different random number seed. The level of variability can be judged from the results shown in the figure. Here, it can be seen that, although diffusivity has an effect on the delay, the variation is only 20% with two orders of magnitude change in

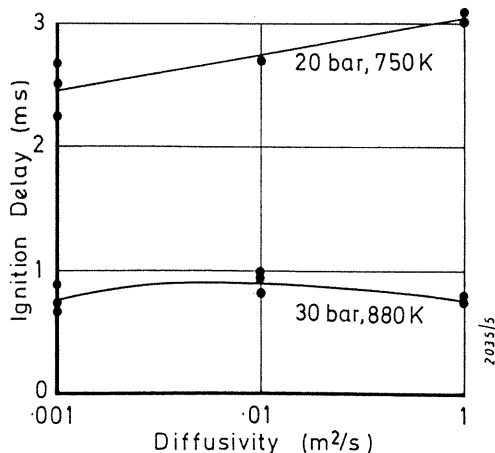


Figure 10. Effect of diffusivity on ignition delay.

diffusivity at the lower pressure and temperature condition and less for the high pressure and temperature case. It may be concluded that, although the delay is sensitive to variations in turbulent transport, the errors introduced into computed ignition delays are not likely to be of great significance providing a reasonable model for the turbulent transport term is provided.

In the light of the above findings, it was not considered worthwhile to try and reproduce the results of (22) with a fixed diffusivity, especially as those results were considered to be dominated by significant numerical diffusion and a fixed diffusivity is, in any case, unrealistic. Figure 11 shows a comparison between the measured and computed variation of ignition delay with bomb pressure and temperature using the  $k - \epsilon$  model to represent turbulence. The 10 bar/670 K case was not run and results from this would not be expected to be meaningful because of extensive impingement in the (computational) bomb before the occurrence of ignition. The computed ignition delays shown in figure 11 are generally lower than those of (22) (see figure 9), in one instance by 30%. The general trends are, however, the same and the overall level of agreement with the experiments is similar. Whilst the agreement could not be described as good, the behaviour is nevertheless encouraging for such a complicated phenomenon. It is expected that further theoretical investigations into the sensitivity of physical parameters on the ignition delay will clarify the controlling mechanisms.

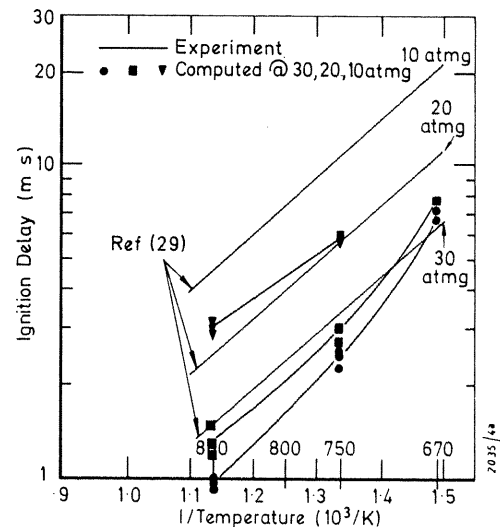


Figure 11. Comparison between computed ignition delay with the measurements of ref.(29).

#### SUMMARY AND CONCLUSIONS

The paper has described a detailed model for diesel combustion in which sub-models for all of the main processes have been provided. An attempt has been made to develop a balanced model, so that the various phenomena are incorporated to the same level of modelling approximation.

The complete model can be considered to consist of three main parts, namely: the mean flow and turbulence; the spray dynamics, heat and mass transfer; and the evolution of the composition and temperature fields. For the last of these, a model based on solving equations for the composition joint pdf and the associated temperature pdf has been developed. To allow a tractable solution, a simplified representation of the pdf has been proposed in which

7 delta functions (or elements) are used to represent the different mixed states of fuel, oxidant and products. The various processes affecting the pdf have been discussed in detail. These include, in addition to transport in physical space, chemical kinetics, mixing and phase change. Separate chemical schemes appropriate to both autoignition and the main combustion have been incorporated.

Validation of different aspects of the air motion and spray models has been briefly described. However, the main focus of the present work has been to assess the ability of the model to calculate the ignition delay for a range of pressure and temperature conditions. In particular, the sensitivity of the calculated delay to turbulent transport, via the effective diffusivity, has been investigated. This both complements and extends the work reported in (22) for the modelling of diesel ignition. It was found that, whilst turbulent transport is important, the errors introduced into computed delays are not likely to be significant, providing a reasonable model for the turbulent transport term is provided.

Work in the immediate future in the continuing development of this model will focus on determining the sensitivity of the ignition delay to other physical parameters, the objective being to identify those areas which are likely to be the most critical to the accurate prediction of the delay.

#### ACKNOWLEDGEMENTS

The author would like to thank Philip Jones for helping with the many computer runs and the Directors of Ricardo Consulting Engineers Ltd. for permission to publish this paper.

#### REFERENCES

1. Ricardo, H.R., "Combustion in Diesel Engines", Proc. IAE, March, 1930.
2. Pope, S.B., "The Probability Approach to the Modelling of Turbulent Reacting Flows", Combustion and Flame, Vol. 27, pp 299-312, 1976.
3. Pope, S.B., "A Monte Carlo Method for the PDF Equations of Turbulent Flow", MIT Energy Lab. Report No. MIT-EL 80-012, 1980.
4. Pope, S.B., "PDF Methods for Turbulent Reactive Flows", Prog. Energy Combust. Sci., Vol. 11, pp 119-192, 1985.
5. Spalding, D.B., "Mixing and Chemical Reaction in Steady Confined Turbulent Flames", 13th Symposium on Combustion, Combustion Institute, pp 649, 1971.
6. Magnussen, B.F. and Hjertager, B.H., "On Mathematical Modelling of Turbulent Combustion with Special Emphasis on Soot Formation and Combustion", 16th Symposium on Combustion, Combustion Institute, pp 719-729, 1976.
7. Bilger, R.W., "The Structure of Turbulent Nonpremixed Flames", Plenary lecture, 22nd Symposium on Combustion, Seattle, 1988.
8. El Tahry, S.H., "k- $\epsilon$  Equation for Compressible Reciprocating Engine Flows", J. Energy, Vol. 7 No. 4, 1983.
9. Dukowicz, J.K., "A Particle-Fluid Numerical Model for Liquid Sprays", Jour. of Comp. Phy., Vol. 35, pp 229-253, 1980.
10. Gosman, A.D. and Johns, R.J.R., "Computer Analysis of Fuel-Air Mixing in Direct-Injection Engines", SAE Trans. and paper 800091, 1980.
11. Borman, G.L. and Johnson, J.H., "Unsteady Vaporisation Histories and Trajectories of Fuel Drops Injected into Swirling Air", SAE 598C, 1962.
12. Shuen, J.S., Chen, L.D. and Faeth, G.M., "Evaluation of a Stochastic Model of Particle Dispersion in a Turbulent Round Jet", AIChE Jour., Vol. 29, No. 1, 1983.
13. O'Rourke, P., "Collective Drop Effects on Vaporizing Liquid Sprays", Ph.D Thesis, Princeton, 1981.
14. O'Rourke, P.J. and Amsden, A.A., "The Tab Method for Numerical Calculation of Spray Droplet Breakup", SAE paper 872089, 1987.
15. Reitz, R.D. and Diwakar, R., "Structure of High-Pressure Fuel Sprays", SAE paper 870598, 1987.
16. Reitz, R., "Atomization and other Breakup Regimes of a Liquid Jet", Ph.D Thesis, Princeton, 1978.
17. Hiroyasu, H. and Kadota, T., "Fuel Droplet Size Distribution in Diesel Combustion Chamber", SAE paper 740715, 1974.
18. Pope, S.B., "An Improved Turbulent Mixing Model", Combustion Science and Technology, Vol. 28, pp 131-145, 1982.
19. Curl, R.L., "Dispersed Phase Mixing: 1. Theory and Effects in Simple Reactors", A.I.Ch.E.J., Vol. 9., pp 175-181, 1963.
20. Schapertons, H. and Lee, W., "Multidimensional Modelling of Knocking Combustion in SI Engines", SAE paper 850502, 1985.
21. Halstead, M.P., Kirsch, L.J. and Quinn, C.P., "The Autoignition of Hydrocarbon Fuels at High Temperatures and Pressures - Fitting of a Mathematical Model", Combustion and Flame, Vol. 30, pp. 45-60, 1977.
22. Theobald, M.A., "Numerical Simulation of Diesel Autoignition", PhD Thesis, MIT, 1986.
23. Westbrook, C.K. and Dryer, F.L., "Simplified Reaction Mechanisms for the Oxidation of Hydrocarbon Fuels in Flames", Combustion Science and Technology, vol. 27, pp. 31-43, 1981.
24. Byrne, G.D. and Hindmarsh, A.C. "Stiff ODE Solvers: A Review of Current and Coming Attractions", J. Comp. Phys., Vol. 70, No.1, pp. 1-62, 1987.
25. Yule, A.J., Mo, S.L., Tham, S.Y. and Aval, S.M., "Diesel Spray Structure", Proc. of the ICLASS-85 conference, paper 11B/2, 1985.
26. Kuniyoshi, H., Tanabe, H., Sato, G.T. and Fujimoto, H., "Investigation on the Characteristics of Diesel Fuel Spray", SAE paper 800968, 1980.
27. Hiroyasu, H. and Kadota, T., "Fuel Droplet Size Distribution in Diesel Combustion Chamber", SAE paper 740715, 1974.
28. Chin, J.S. and Lefebvre, A.H., "Steady-State Evaporation Characteristics of Hydrocarbon Fuel Drops", AIAA Jour., Vol. 21, No. 10, pp 1437-1443, 1983.
29. Igura, S., Kadota, T. and Hiroyasu, H., "Spontaneous Ignition Delay of Fuel Sprays in High Pressure Gaseous Environments", Translated from JSME, Vol. 41, No. 345, pp. 1559-1566, 1975.